

# Single-hole properties in the $t$ - $J$ and strong-coupling models

B. M. Elrick\* and A. E. Jacobs\*

*Department of Physics, University of Toronto, Toronto, Ontario, Canada M5S 1A7*

(November 19, 2018)

We report numerical results for the single-hole properties in the  $t$ - $J$  model and the strong-coupling approximation to the Hubbard model in two dimensions. Using the hopping basis with over  $10^6$  states we discuss (for an infinite system) the bandwidth, the leading Fourier coefficients in the dispersion, the band masses, and the spin-spin correlations near the hole. We compare our results with those obtained by other methods. The band minimum is found to be at  $(\pi/2, \pi/2)$  for the  $t$ - $J$  model for  $0.1 \leq t/J \leq 10$ , and for the strong-coupling model for  $1 \leq t/J \leq 10$ . The bandwidth in both models is approximately  $2J$  at large  $t/J$ , in rough agreement with loop-expansion results but in disagreement with other results. The strong-coupling bandwidth for  $t/J \gtrsim 6$  can be obtained from the  $t$ - $J$  model by treating the three-site terms in first-order perturbation theory. The dispersion along the magnetic zone face is flat, giving a large parallel/perpendicular band mass ratio.

PACS numbers: 71.27.+a, 74.25.Jb, 75.10.Jm

## I. INTRODUCTION

Anderson's suggestion<sup>1</sup> that the copper-oxygen planes of the high-temperature superconductors<sup>2</sup> are strongly correlated systems has sparked renewed interest in the two-dimensional Hubbard model. Much of our understanding of the strong-coupling limit of the model, and the related  $t$ - $J$  model, has been obtained by numerical work (reviewed in Ref. 3). Although the single-hole properties have been studied extensively, exact-diagonalization studies of small systems are hindered by large finite-size effects in the parameter region of interest, and Monte-Carlo studies of larger systems are hindered by the minus-sign problem; other methods have also been used, but there is still no general agreement on these properties, particularly for  $t/J$  values in the physical region. For this reason, we have studied the single-hole properties using the hopping basis of Trugman<sup>4,5</sup> and compared them with results obtained by other methods.

In the limit  $U \gg t$ , the Hubbard Hamiltonian can be approximated by the strong-coupling Hamiltonian<sup>6</sup>  $H_{sc} = H_{t-J} + H_3$ ; this differs from the  $t$ - $J$  Hamiltonian  $H_{t-J}$  (which has its own justification) by the three-site terms in  $H_3$ :

$$H_{t-J} = -t \sum_{i,\delta,\sigma} c_{i+\delta,\sigma}^\dagger c_{i,\sigma} + J \sum_{\langle ij \rangle} (\mathbf{S}_i \cdot \mathbf{S}_j - \frac{1}{4} n_i n_j), \quad (1)$$

$$H_3 = -\frac{J}{4} \sum_{i,\sigma} \sum_{\delta,\delta'} (c_{i+\delta,\sigma}^\dagger c_{i,-\sigma}^\dagger c_{i,-\sigma} c_{i+\delta',\sigma} - c_{i+\delta,-\sigma}^\dagger c_{i,\sigma}^\dagger c_{i,-\sigma} c_{i+\delta',\sigma}); \quad (2)$$

here sites  $i + \delta$  and  $i + \delta'$  are distinct nearest neighbors of site  $i$ ,  $\langle ij \rangle$  are nearest-neighbor pairs, and  $J = 4t^2/U$ . The  $t$ - $J$  and strong-coupling Hamiltonians operate in the reduced Hilbert space with no doubly occupied sites; this restriction is implicit in the above. Validity of the strong-coupling approximation requires  $U \gg t$ ; the parameter range believed appropriate to the high-temperature superconductors is  $2 < t/J < 10$ , or  $8 < U/t < 40$ . We

present results for the  $t$ - $J$  model in the region  $0.1 \leq t/J \leq 10$  and for the strong-coupling model in the region  $1 \leq t/J \leq 10$ .

The single-hole properties in the  $t$ - $J$  and strong-coupling models have been studied previously, the first having received more attention. Methods include exact-diagonalization studies of small lattices<sup>7-14</sup>, studies of infinite lattices using a restricted basis set<sup>4,5,15-18</sup>, Monte-Carlo methods<sup>19-25</sup>, and other methods<sup>26-34</sup>. Properties discussed include the ground-state energy, the bandwidth, the dispersion, the band masses, the nearest-neighbor spin-spin correlations and the spectral function. As well, there is an extensive literature on the Hubbard model itself, including recent finite-temperature Monte-Carlo results<sup>35-37</sup>.

This paper studies the one-hole properties on an infinite lattice, using a restricted basis set (in effect a variational method). Section II describes the basis, and Sections IV-VI give results for the bandwidth, the dispersion, the band masses, and the nearest-neighbor spin-spin correlations respectively. For both models, the band minimum is at  $\mathbf{k} = (\pi/2, \pi/2)$  and the maximum at  $\mathbf{k} = (0, 0)$  for the  $t/J$  values investigated. The bandwidth is approximately  $2J$  at large  $t/J$ , in agreement with loop-expansion results<sup>28,29,32</sup> and in disagreement with variational Monte-Carlo results<sup>21</sup>. At large  $t/J$ , the effects of three-site terms on the bandwidth are well described by first-order perturbation theory using the  $t$ - $J$  ground-state wavefunction; that is, the three-site terms appear to have little effect on the ground-state wavefunction at large  $t/J$ . The band mass parallel to the zone face is much larger than the perpendicular mass. The spin-spin correlations near the hole are reduced relative to the starting state, but remain antiferromagnetic.

## II. HOPPING BASIS

We study a system of  $N - 1$  electrons on a square lattice of  $N$  sites with periodic boundary conditions; the

Hilbert space is restricted to the  $S_z = 1/2$  sector with no doubly occupied sites. We use the same basis for both models, namely the hopping basis<sup>4,5</sup> which has been used previously<sup>4,5,15–18</sup>. This method allows the study of infinite systems (eliminating finite-size effects), but only certain properties, like the bandwidth and the band masses, can be studied.

In zeroth order, the basis (denoted  $B_0$ ) consists of a single state (denoted  $|cN\rangle$ ), the Néel state with a missing down-spin electron. Higher-order bases are generated by repeatedly applying the  $t$  term in the Hamiltonian (which hops the hole to a nearest-neighbor site). The first-order basis  $B_1$  contains the  $|cN\rangle$  state plus the four states generated by hopping the hole. The  $n$ -th order basis  $B_n$  consists of the states in the basis  $B_{n-1}$  plus those generated by applying the hopping operator to the states in the difference  $B_{n-1} - B_{n-2}$ . The basis size (values are given in Table I) grows exponentially with order. The hopping basis, which emphasizes states differing from the  $|cN\rangle$  state only near the hole, cannot give a good value of the ground-state energy (because, for example, it does not generate spin interchanges far from the hole in reasonable order); the expectation is that it describes well properties like the dispersion and the nearest-neighbor spin-spin correlations near the hole.

We have used the bases from  $B_6$  to  $B_{13}$  for most quantities, going to such large bases because some properties were still changing significantly; even with basis  $B_{13}$  ( $\sim 2 \times 10^6$  states), however, some properties are incompletely converged. Various extrapolation schemes were considered but judged unreliable, and so we usually present values for the three largest bases to provide an estimate of the error due to the truncation of the basis.

The system size ( $16 \times 16$ ; the lattice constant  $a$  is unity) is effectively infinite since there are no paths which wrap around the system even in 13-th order. Since the hole moves in an antiferromagnetic background, the Brillouin zone is reduced to the square formed by the points  $(\pm\pi, 0)$  and  $(0, \pm\pi)$ . The symmetries of the lattice reduce the independent part of the Brillouin zone to the triangle with corners at  $(0, 0)$ ,  $(\pi, 0)$ , and  $(\pi/2, \pi/2)$ , denoted  $\Gamma$ ,  $\mathbf{M}$ , and  $\mathbf{S}$  respectively. Each state  $|n\rangle$  in the basis is a Bloch state, an eigenstate of the translation operator corresponding to an allowed value of the momentum. For each basis, and each value of the momentum  $\mathbf{k}$ , the lowest eigenvalue and eigenvector were found using a conjugate-gradient method to minimize the function  $\langle\Psi|H|\Psi\rangle/\langle\Psi|\Psi\rangle$  with respect to the expansion coefficients in  $|\Psi\rangle = \sum_n a_n |n\rangle$ ; this method is reported to converge more rapidly than others commonly used<sup>38</sup>, but gives the eigenvector to only single precision. Where necessary, the eigenvector was improved by a Lanczos method.

The dispersion (in the energy as a function of  $\mathbf{k}$ ) results from several processes. The Trugman paths<sup>4,5</sup> translate the hole to a next-nearest-neighbor site or a third-nearest-neighbor site on the same sub-lattice, restoring the original configuration. In the lowest-order path, the hole hops six times around the smallest square to a next-

nearest-neighbor site; as a result, matrix elements like  $\langle B_2 | c_{i+\delta,\sigma}^\dagger c_{i,\sigma} | B_3 \rangle$  are momentum-dependent. Momentum dependence can also arise from the  $J$  term in  $H$ ; for example, the basis  $B_2$  contains states with the hole translated by  $2a$  and a pair of flipped spins, and so matrix elements like  $\langle B_0 | \mathbf{S}_i \cdot \mathbf{S}_j | B_2 \rangle$  depend on  $\mathbf{k}$ . The results show odd-even effects in the order of the basis; as the basis size increases, Trugman paths of higher order, and also states differing from the starting state by nearest-neighbor spin interchanges, are generated.

Related bases were also studied, in an effort to determine which states are important for the hole properties. The hopping basis can be described symbolically as  $B_n = \sum_{k=0}^n h^k |cN\rangle$  where  $h$  is the hole hopping operator. We define also operators  $\mathcal{S}_8$ ,  $\mathcal{S}_{12}$  and  $\mathcal{S}_{20}$ ; the first scrambles the 8 spins at distances  $a$  and  $\sqrt{2}a$  from the hole (giving 70 states when operating on the  $|cN\rangle$  state), the second these spins plus the four at distance  $2a$ , and the third the 20 spins inside a  $5 \times 5$  square minus the four corner sites. If hole properties like the bandwidth are determined primarily by configurations which differ from the  $|cN\rangle$  state only near the hole, then the bases  $\sum_k h^k \mathcal{S}_m |cN\rangle$ , or (likely better)  $\mathcal{S}_m \sum_k h^k |cN\rangle$ , should converge more rapidly than the hopping basis; we find the opposite: when the bandwidth is plotted against the inverse of the log of the basis size, these modified bases behave like the hopping basis, except that properties are shifted toward larger basis sizes. We considered also two other bases, both of which reduce the importance of string states (in which the hole wanders without looping): (i) the basis  $\sum_k M_m h^k |cN\rangle$  where the operator  $M_m$  removes states in which the Manhattan displacement ( $|x| + |y|$ ) of the hole relative to its initial position is greater than  $ma$ , and (ii) the basis  $\sum_{k=0}^\infty (I_n h)^k |cN\rangle$ , where the operator  $I_n$  removes states with more than  $n$  “bad bonds” (that is, it filters states according to their Ising energy relative to the  $|cN\rangle$  state; the limit  $\infty$  means that the hop-filter combination is applied until the basis no longer grows, for given  $n$ ). Neither the Manhattan nor the Ising filters improved the convergence. We conclude from these numerical experiments that the single-hole properties are determined not so much by the spin configurations near the hole as by loop and string paths. It appears that the hopping basis, whether in its original form or in the modified forms we have investigated, is capable of only limited accuracy even if carried to very high order.

### III. BANDWIDTH

Because the lattice is effectively infinite, the lowest energy can be found for any  $\mathbf{k}$ . For both models, we found  $E(\mathbf{k})$  at 81 independent  $\mathbf{k}$  values of the form  $(2\pi n/L, 2\pi m/L)$  with  $n$  and  $m$  integers and  $L = 32$ , for  $t/J$  values in the range  $0.1 \leq t/J \leq 10$  for the  $t$ - $J$  model and in the range  $1 \leq t/J \leq 10$  for the strong-

coupling model (for which the lower values of  $t/J$  are of little interest).

For the  $t$ - $J$  model, the energy is a minimum at  $\mathbf{k} = \mathbf{S}$  (and a maximum at  $\mathbf{\Gamma}$ ) for  $0.1 \leq t/J \leq 10$ , for all bases used ( $B_6$  to  $B_{13}$ ), in agreement with all previous work.

For the strong-coupling model, the energy is also a minimum at  $\mathbf{k} = \mathbf{S}$  (and a maximum at  $\mathbf{\Gamma}$ ) for all  $t/J$  in the range  $1.0 \leq t/J \leq 10$ , but only for the largest bases at small  $t/J$ ; this result disagrees with predictions (based on fits to exact-diagonalization results for small systems<sup>13</sup>) that the minimum is at  $\mathbf{M}$  for  $t/J \leq 5$ . For the smaller bases, particularly for the smaller values of  $t/J$ , the minimum can be at  $\mathbf{M}$  or elsewhere along the zone face; for example, the minimum is at  $\mathbf{S}$  only in 11-th order and higher for  $t/J = 1$ .

Figure 1 plots the bandwidth  $W = E(\mathbf{\Gamma}) - E(\mathbf{S})$  for both models as found using the bases  $B_{11}$ ,  $B_{12}$ , and  $B_{13}$ . The convergence is good for the  $t$ - $J$  model at all  $t/J$  investigated; it is moderately good for the strong-coupling model at larger  $t/J$ , but worsens at smaller  $t/J$ . The  $t$ - $J$  bandwidth is approximately  $t$  for  $t/J < 2$  and  $2J$  for  $t/J > 2$ , but decreases weakly at large  $t/J$ . The strong-coupling bandwidth is also about  $2J$  (though about 20% larger) and also decreases as  $t/J$  increases. The hopping-basis results are incompletely converged, however; the bandwidth is still increasing with basis size, and the trend is greater at larger  $t/J$ . It is possible then that the slight decrease which we find is due to the finite size of the hopping basis.

Figure 2 compares our values for the  $t$ - $J$  bandwidth with those obtained by other methods; major differences occur in the physical region  $t/J > 2$ . The hopping-basis results agree best with loop-expansion results<sup>28,29,32</sup> and poorly with variational Monte-Carlo results<sup>21</sup> (for unknown reasons); the  $4 \times 4$  exact-diagonalization results<sup>14</sup> at large  $t/J$  are unreliable due to finite-size effects. Our results at large  $t/J$  are qualitatively consistent with the mean-field result<sup>39</sup>  $W \approx 4J$  for strong coupling.

From Figure 1, the normalized bandwidth difference  $(W_{sc} - W_{t-J})/J$  is almost independent of  $t/J$  for  $t/J \gtrsim 4$ . Since  $(H_{sc} - H_{t-J})/J = H_3/J$  has no explicit dependence on  $t$  or  $J$ , this suggests treating the three-site terms as a perturbation to the  $t$ - $J$  model. The error in the first-order result for the bandwidth difference  $\Delta W_1 = \Delta E_1(\mathbf{\Gamma}) - \Delta E_1(\mathbf{M})$ , where  $\Delta E_1(\mathbf{k}) = \langle \Psi_{t-J} | H_3 | \Psi_{t-J} \rangle(\mathbf{k})$ , is less than 2% at  $t/J = 10$  and  $t/J = 8$ , but is much larger at smaller  $t/J$  (52% at  $t/J = 4$ ). Of course the estimate for the strong-coupling bandwidth itself is much better (errors are 0.3%, 0.3%, and 11% at  $t/J = 10, 8$ , and 4). It appears then that the three-site terms can be treated in first order for  $t/J \gtrsim 6$ .

Further investigation revealed that the first-order estimates of the energy at  $\mathbf{S}$  are excellent;  $(\langle H_{sc} \rangle_{t-J} - E_{sc})/W_{sc}$  is 0.1%, 0.09%, 0.06% and 0.04% at  $t/J = 10, 8, 4$ , and 1 respectively; the corresponding values at  $\mathbf{\Gamma}$  are 0.4%, 0.4%, 11% and 41%. For unknown reasons, at intermediate  $t/J$  values the three-site terms appear to affect the  $\mathbf{\Gamma}$  ground state strongly and the  $\mathbf{M}$  ground state

very weakly.

## IV. DISPERSION

The Fourier coefficients  $a_{lm}$  defined by

$$E(\mathbf{k}) = \sum_{l,m=0}^{L/2} a_{lm} \cos lk_x \cos mk_y \quad (3)$$

are easily obtained by inversion from the energy as a function of  $\mathbf{k}$ . The symmetries of the lattice give  $a_{lm} = a_{ml}$ , and  $a_{lm} = 0$  for  $l + m$  odd. The independent coefficients are then the 81  $a_{lm}$  with  $0 \leq l \leq 16$ ,  $0 \leq m \leq l$ , and  $l + m$  even. The coefficient  $a_{00}$  depends strongly on the order of the basis, as more states important for the ground-state energy are generated; it affects none of our results since we look only at quantities (like the dispersion) which depend on energy differences.

Of the other coefficients,  $a_{11}$  and  $a_{20}$  (both positive) are the largest, with the ratio  $a_{20}/a_{11}$  less than about 0.6 for both models for the range of  $t/J$  values studied. The remaining coefficients are less than about  $0.1a_{11}$  in magnitude for both models at the  $t/J$  values studied. Figures 3 and 4 plot the two leading coefficients as functions of  $t/J$  for the two models. The convergence is of course qualitatively the same as for the bandwidth, good for the  $t$ - $J$  model at all  $t/J$  and for the strong-coupling model for  $t/J \gtrsim 4$ , but increasingly poor for the latter with decreasing  $t/J$ .

At large  $t/J$ , the values  $a_{20}/J$  are almost independent of  $t/J$ , whereas the coefficients  $a_{11}/J$  decrease with increasing  $t/J$ . The strong-coupling coefficients are larger than the  $t$ - $J$  coefficients, reflecting the enhanced mobility due to the three-site terms. Also, at larger  $t/J$ , the difference  $(a_{20}/J)_{sc} - (a_{20}/J)_{t-J}$  for the two models is almost independent of  $t/J$ , as is the difference in the values of  $a_{11}/J$ , for the reason discussed in Section III. Figures 3 and 4 also plot other results<sup>28,29</sup> for the  $t$ - $J$  Fourier coefficients; the agreement is as expected from Section III. Recent Monte-Carlo results<sup>25,23</sup>, available only at  $t/J = 2.5$ , are about 25% higher than ours.

## V. BAND MASSES

The band masses at the band minimum, which is at  $\mathbf{S}$  for both models in the region  $1 \leq t/J \leq 10$ , are defined in terms of the second derivatives of  $E(\mathbf{k})$  with respect to  $\mathbf{k}$ :

$$m_{\mu\nu} = \hbar^2 \left( \frac{\partial^2 E(\mathbf{k})}{\partial k_\mu \partial k_\nu} \right)^{-1}. \quad (4)$$

The masses were obtained by calculating  $E(\mathbf{k})$  at additional points near  $\mathbf{S}$  and using finite-difference approximations for the derivatives. Figures 5 and 6 give results

for the masses perpendicular and parallel to the zone face respectively, in units of the bare mass  $m_0 = \hbar^2/2t$ . The parallel mass is much larger than the perpendicular mass, as found previously<sup>15,18,13,29,28,25</sup>.

The perpendicular mass is well converged for both models. For the  $t$ - $J$  model,  $m_{\perp}/m_0$  is almost linear in  $t/J$  at large  $t/J$ , but flattens out at small  $t/J$ . For the strong-coupling model,  $m_{\perp}/m_0$  is almost proportional to  $t/J$ ; the smaller effective mass reflects again the increased hole mobility relative to that in the  $t$ - $J$  model.

The parallel mass is much more poorly converged, especially at smaller  $t/J$ ; even at  $t/J = 10$  (the most favorable value), the masses change by over 5% between the bases  $B_{12}$  and  $B_{13}$ . The poor convergence results because the energies are nearly independent of  $\mathbf{k}$  (the mass is large). For large  $t/J$ , though, it appears that  $m_{\parallel}/m_0$  increases only weakly with  $t/J$  for both models and that the two models have the same parallel mass.

Figures 5 and 6 also give the results from Ref. 29, derived from their dispersion results (Table II of Ref. 29) using the free mass  $m_0 = \hbar^2/2t$ , rather than the effective masses of their Table III. The difference is due in part to a genuinely different dispersion, but part of it arises because they used only two components in the Fourier expansion (the parallel mass, being large, is particularly sensitive to small changes in the energy).

## VI. SPIN-SPIN CORRELATIONS

Figures 7 and 8 show the nearest-neighbor spin-spin correlation  $\langle \mathbf{S}_i \cdot \mathbf{S}_j \rangle$  for pairs of sites  $i$  and  $j$  near the hole, for the  $t$ - $J$  model and strong-coupling model respectively. The momentum is  $\mathbf{k} = \mathbf{S}$  (the band minimum),  $t/J = 2.5$ , and the basis is  $B_{13}$ . In the units of  $\hbar^2 = 1$  used, the spin-spin correlation is -0.75 for a singlet pair of spins, 0.25 for a triplet pair, and -0.25 for a Néel pair. The correlations are antiferromagnetic, and moderately less than in the starting state. The “cigar” polaron in Figures 7 and 8 is well known from other studies<sup>40,8,11,16</sup>.

## ACKNOWLEDGMENTS

This research was supported by the Natural Sciences and Engineering Research Council of Canada. Computations were done on a Kendall Square Research 1-32 computer provided by University of Toronto Instructional and Research Computing; we are grateful to UTIRC staff for aid in making efficient use of the parallel architecture.

---

\* e-mail addresses: elrick@physics.utoronto.ca and jacobs@physics.utoronto.ca

- <sup>1</sup> P.W. Anderson, *Science* **235**, 1196 (1987).
- <sup>2</sup> J.G. Bednorz and K.A. Müller, *Z. Phys. B* **64**, 189 (1986).
- <sup>3</sup> E. Dagotto, *Rev. Mod. Phys.* **66**, 763 (1994).
- <sup>4</sup> S.A. Trugman, *Phys. Rev. B* **37**, 1597 (1988).
- <sup>5</sup> S.A. Trugman, *Phys. Rev. B* **41**, 892 (1990).
- <sup>6</sup> A.B. Harris and R.V. Lange, *Phys. Rev.* **157**, 295 (1967); J.E. Hirsch, *Phys. Rev. Lett.* **54**, 1317 (1985).
- <sup>7</sup> E. Kaxiras and E. Manousakis, *Phys. Rev. B* **37**, 656 (1988).
- <sup>8</sup> E. Dagotto, A. Moreo, and T. Barnes, *Phys. Rev. B* **40**, 6721 (1989).
- <sup>9</sup> E. Dagotto, R. Joynt, A. Moreo, S. Bacci, and E. Gagliano, *Phys. Rev. B* **41**, 9049 (1990).
- <sup>10</sup> J. Bonča, P. Prelovšek, and I. Sega, *Phys. Rev. B* **39**, 7074 (1989).
- <sup>11</sup> V. Elser, D.A. Huse, B.I. Shraiman, and E.D. Siggia, *Phys. Rev. B* **41**, 6715 (1990).
- <sup>12</sup> H. Röder, V. Waas, H. Fehske, and H. Büttner, *Phys. Rev. B* **43**, 6284 (1991).
- <sup>13</sup> H. Fehske, V. Waas, H. Röder, and H. Büttner, *Phys. Rev. B* **44**, 8473 (1991).
- <sup>14</sup> B.M. Elrick, M.D. Kovarik, A.E. Jacobs, and W.G. Macready, *Phys. Rev. B* **47**, 6004 (1993).
- <sup>15</sup> J. Inoue and S. Maekawa, *J. Phys. Soc. Jpn.* **59**, 2110 (1990).
- <sup>16</sup> J. Inoue and S. Maekawa, *J. Phys. Soc. Jpn.* **59**, 3467 (1990).
- <sup>17</sup> J. Inoue, K. Iiyama, S. Kobayashi, and S. Maekawa, *Phys. Rev. B* **49**, 6213 (1994).
- <sup>18</sup> W.G. Macready and A.E. Jacobs, *Phys. Rev. B* **44**, 5166 (1991).
- <sup>19</sup> M. Boninsegni and E. Manousakis, *Phys. Rev. B* **43**, 10353 (1991).
- <sup>20</sup> M. Boninsegni and E. Manousakis, *Phys. Rev. B* **46**, 560 (1992).
- <sup>21</sup> M. Boninsegni and E. Manousakis, *Phys. Rev. B* **45**, 4877 (1992).
- <sup>22</sup> E. Dagotto and J.R. Schrieffer, *Phys. Rev. B* **43**, 8705 (1991).
- <sup>23</sup> T. Giamarchi and C. Lhuillier, *Phys. Rev. B* **47**, 2775 (1993).
- <sup>24</sup> T. Barnes and M.D. Kovarik, *Phys. Rev. B* **47**, 11247 (1993).
- <sup>25</sup> E. Dagotto, A. Nazarenko, and M. Boninsegni, *Phys. Rev. Lett.* **73**, 728 (1994).
- <sup>26</sup> S. Schmitt-Rink, C.M. Varma, and A.E. Ruckenstein, *Phys. Rev. Lett.* **60**, 2793 (1988).
- <sup>27</sup> C.L. Kane, P.A. Lee, and N. Read, *Phys. Rev. B* **39**, 6880 (1989).
- <sup>28</sup> F. Marsiglio, A.E. Ruckenstein, S. Schmitt-Rink, and C.M. Varma, *Phys. Rev. B* **43**, 10882 (1991). The definition of  $J$  in this article differs by a factor of 2 from the usual definition.
- <sup>29</sup> G. Martínez and P. Horsch, *Phys. Rev. B* **44**, 317 (1991).
- <sup>30</sup> Z. Liu and E. Manousakis, *Phys. Rev. B* **44**, 2414 (1991).
- <sup>31</sup> Z. Liu and E. Manousakis, *Phys. Rev. B* **45**, 2425 (1992).
- <sup>32</sup> Z. Liu and E. Manousakis, *Phys. Rev. B* **51**, 3156 (1995).
- <sup>33</sup> O.P. Sushkov, *Solid State Comm.* **83**, 303 (1992).
- <sup>34</sup> O.P. Sushkov, *Phys. Lett. A* **162**, 199 (1991).
- <sup>35</sup> N. Bulut, D.J. Scalapino, and S.R. White, *Phys. Rev. Lett.*

**72**, 705 (1994).

<sup>36</sup> N. Bulut, D.J. Scalapino, and S.R. White, Phys. Rev. Lett. **73**, 748 (1994).

<sup>37</sup> N. Bulut, D.J. Scalapino, and S.R. White, Phys. Rev. B **50**, 7215 (1994).

<sup>38</sup> M.P. Nightingale, V.S. Viswanath, and G. Müller, Phys. Rev. B **48**, 7696 (1993).

<sup>39</sup> J.R. Schrieffer, X.G. Wen, and S.C. Zhang, Phys. Rev. B **39**, 11663 (1989).

<sup>40</sup> W.P. Su, Phys. Rev. B **37**, 9904 (1988).

TABLE I. Number of states in the hopping basis versus order of the basis.

<i>Order of Basis</i>	<i>Number of states</i>	<i>Order of Basis</i>	<i>Number of states</i>
0	1	8	9 786
1	5	9	27 990
2	17	10	80 196
3	49	11	228 196
4	141	12	650 022
5	405	13	1 842 326
6	1 177	14	5 225 938
7	3 389		

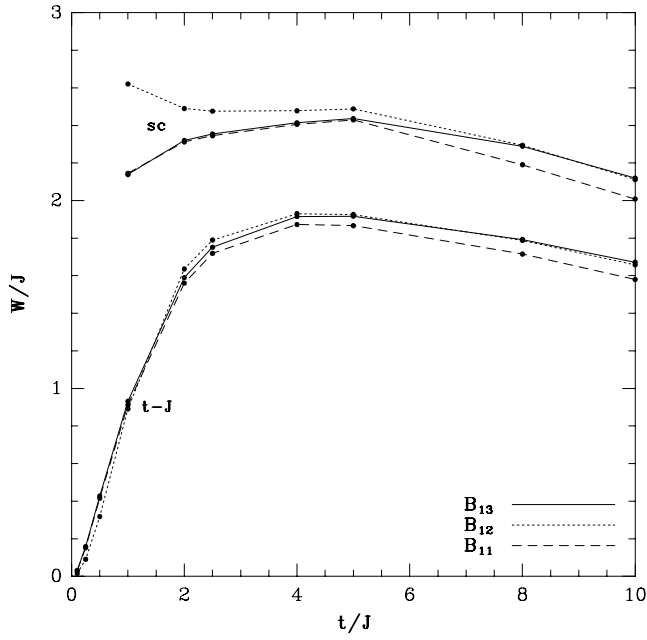


FIG. 1. Bandwidth  $W$ , in units of  $J$ , for the  $t$ - $J$  and strong-coupling (sc) models as functions of  $t/J$  for the three largest bases used. The lines merely connect the points, here and in following Figures.

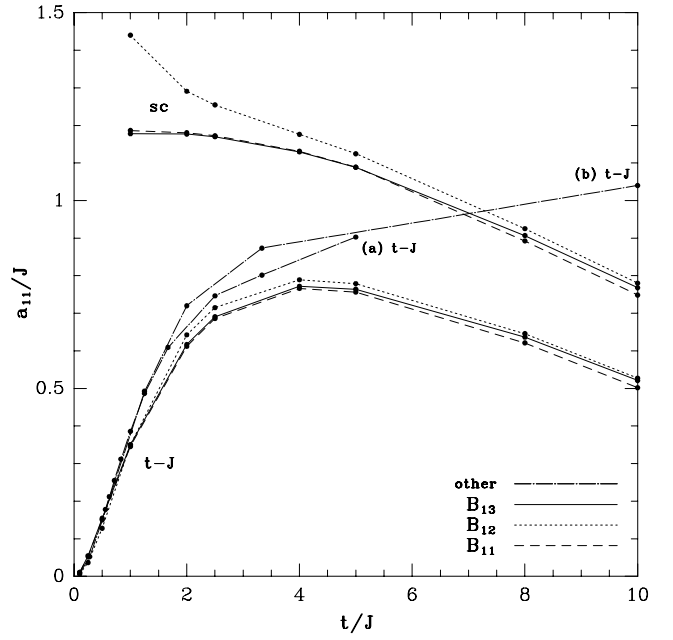


FIG. 3. The leading Fourier coefficient  $a_{11}$ , in units of  $J$ , for the  $t$ - $J$  and strong-coupling (sc) models as functions of  $t/J$  for the three largest bases used. The dot-dash lines give other results for the  $t$ - $J$  model: (a) Ref. 28 and (b) Ref. 29.

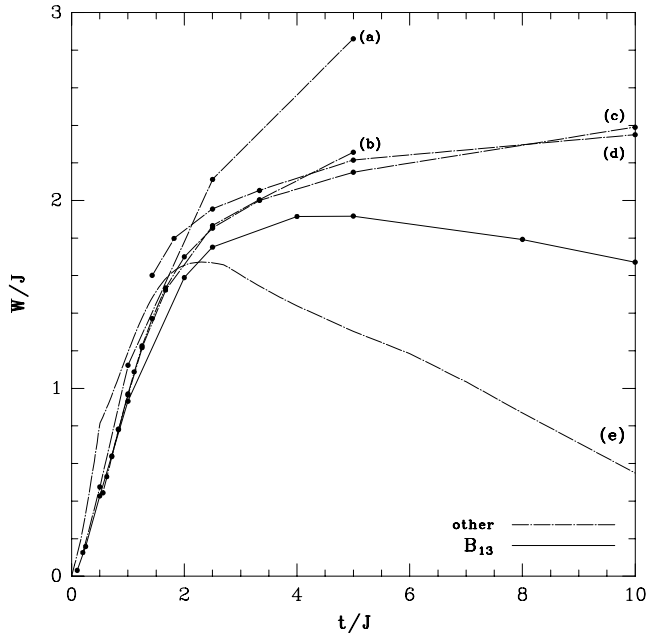


FIG. 2. Bandwidth  $W$ , in units of  $J$ , for the  $t$ - $J$  model as functions of  $t/J$ . The solid line gives the hopping-basis results (for the basis  $B_{13}$ ) and the dot-dash lines other results: (a) Ref. 21, (b) Ref. 28, (c) Ref. 29, (d) Ref. 32, and (e) Ref. 14.

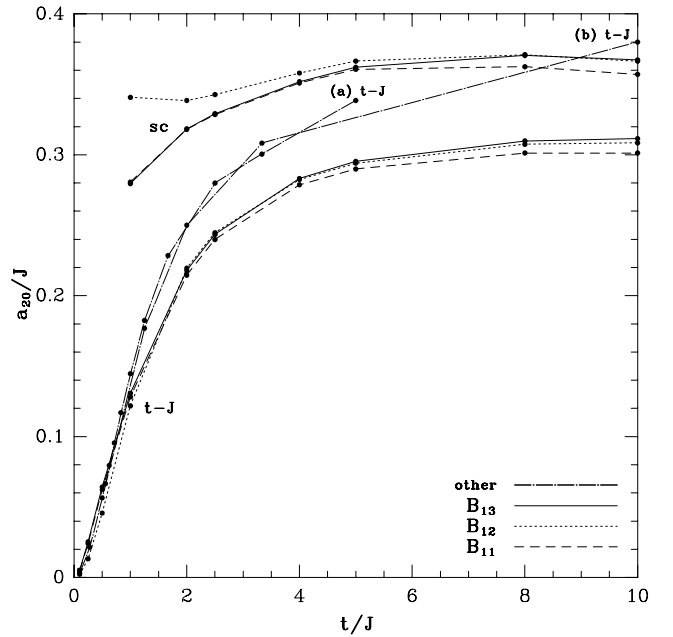


FIG. 4. The second leading Fourier coefficient  $a_{20}$ , in units of  $J$ , for the  $t$ - $J$  and strong-coupling (sc) models as functions of  $t/J$  for the three largest bases used. The dot-dash lines give other results for the  $t$ - $J$  model: (a) Ref. 28 and (b) Ref. 29.

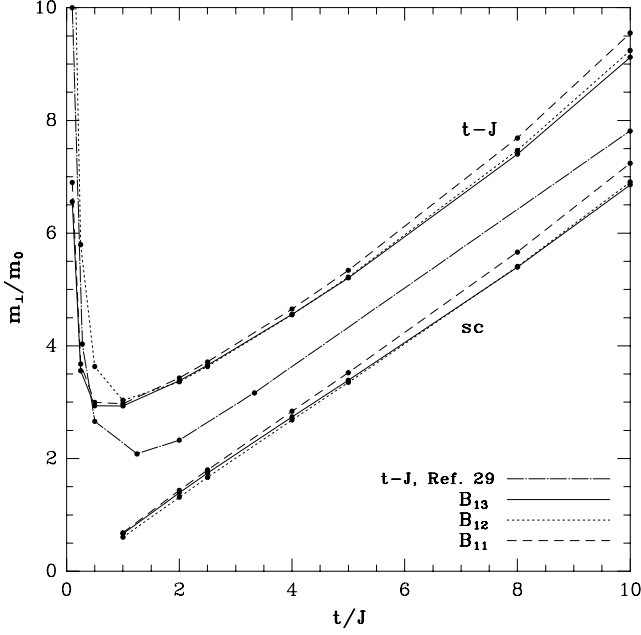


FIG. 5. Band mass perpendicular to the magnetic zone face at the band minimum  $\mathbf{k} = \mathbf{S}$ , in units of the free band mass  $m_0 = \hbar^2/2t$ , for the  $t$ - $J$  and strong-coupling (sc) models as functions of  $t/J$ . The dot-dash line gives the  $t$ - $J$  results of Ref. 29.

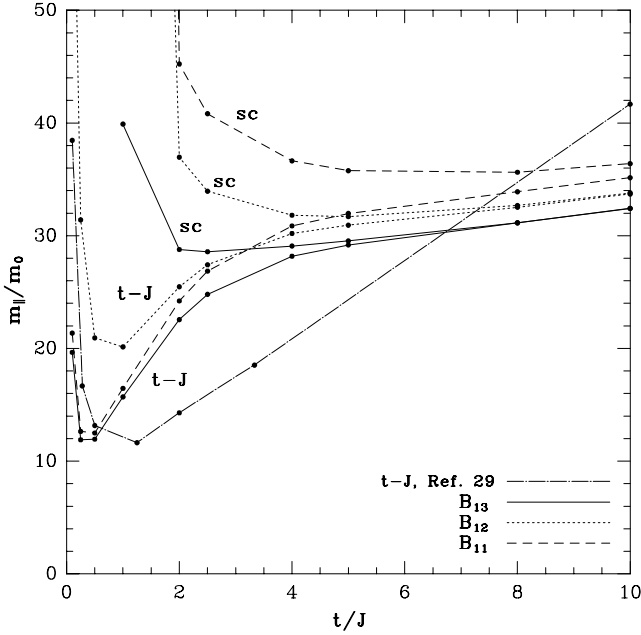


FIG. 6. Band mass parallel to the magnetic zone face at the band minimum  $\mathbf{k} = \mathbf{S}$ , in units of the free band mass  $m_0 = \hbar^2/2t$ , for the  $t$ - $J$  and strong-coupling (sc) models as functions of  $t/J$ . The dot-dash line gives the  $t$ - $J$  results of Ref. 29.

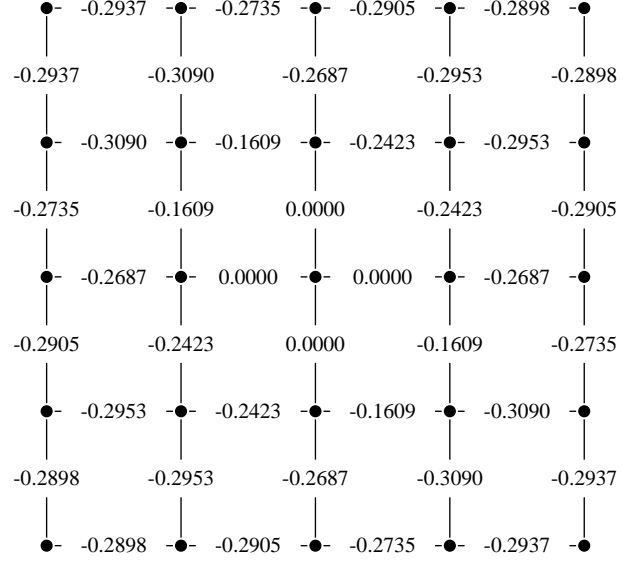


FIG. 7. Nearest-neighbor spin-spin correlations, in units of  $\hbar^2$ , for the  $t$ - $J$  model at the band minimum  $\mathbf{k} = \mathbf{S}$  for  $t/J = 2.5$  using the basis  $B_{13}$ .

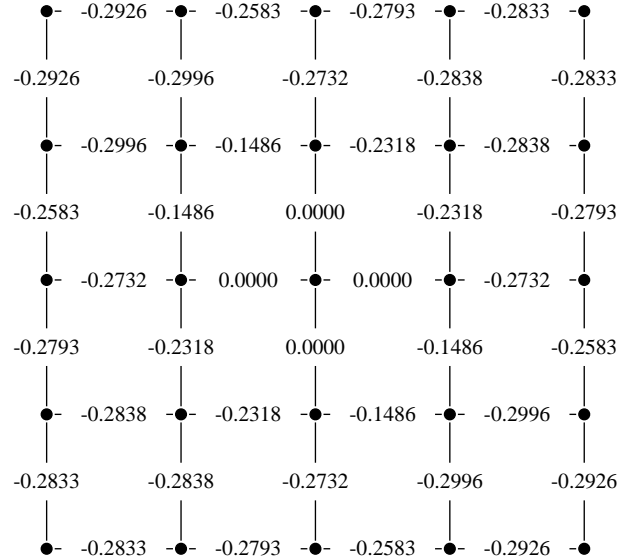


FIG. 8. Nearest-neighbor spin-spin correlations, in units of  $\hbar^2$ , for the strong-coupling model at the band minimum  $\mathbf{k} = \mathbf{S}$  for  $t/J = 2.5$  using the basis  $B_{13}$ .